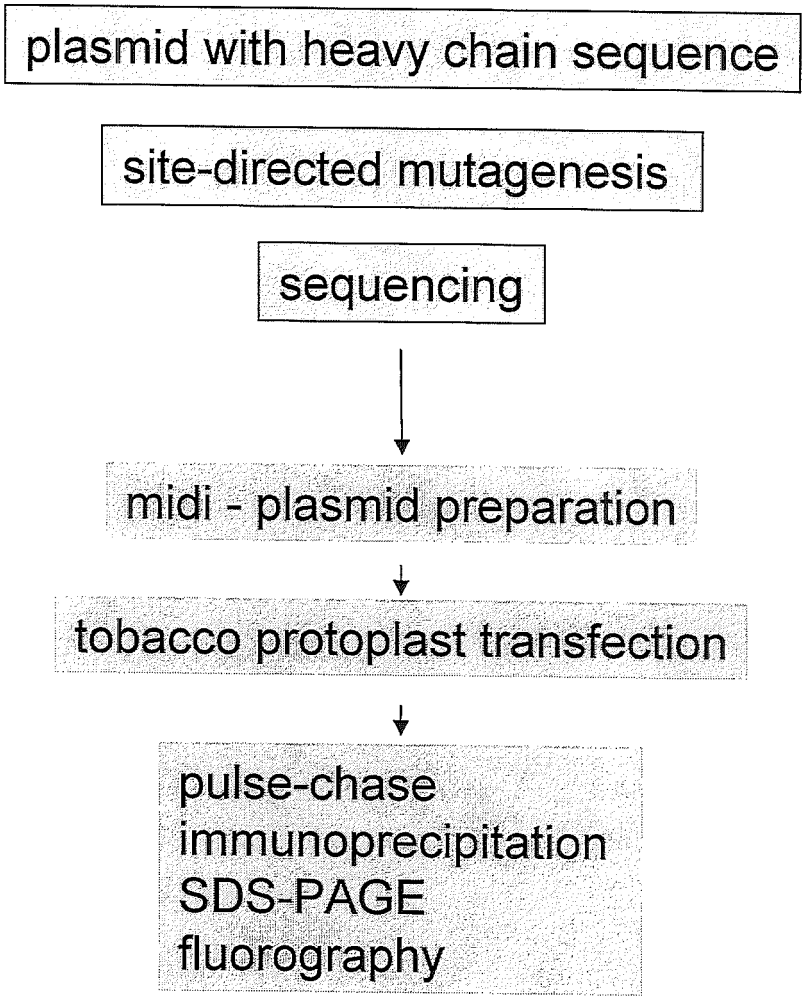

Page 12, last paragraph through Page 16, line 21

Page 16, lines 25-32

Page 16, line 33 through Page 17, line 17

EXHIBIT A

mechanism of NA release from rat cerebral-cortex synaptosomes. Because immunocytochemical studies have shown that B-50 is found in synapses throughout the brain[21,22], B-50 could be more generally involved in transmitter release. Three lines of evidence suggest that the phosphorylation of B-50 by PKC is essential for stimulus–secretion coupling during transmitter release: (1) phorbol esters that directly activate PKC enhance the release of a variety of neurotransmitters[1–4]; (2) by using an antibody-independent approach, we have previously shown that depolarization-induced neurotransmitter release from non-permeabilized synaptosomes and hippocampal slices is closely correlated with a PKC-mediated increase in B-50 phosphorylation[18,23]; and (3) here we have shown that anti-B-50 IgG inhibits B-50 phosphorylation as well as Ca^{2+}-dependent transmitter release. If B-50 phosphorylation by PKC is indeed involved in the mechanism of transmitter release, then a long-term increase in PKC-mediated B-50 phosphorylation[7,17] could be one of the mechanisms underlying the increase in the release of glutamate that occurs during long-term potentiation[5–7,24,25].

In view of the localization of B-50 at the inner leaflet of the plasma membrane[21,26], we suggest that B-50 is involved in the regulation of vesicle fusion with the plasma membrane, a process in which the vesicle-associated protein synapsin I (a substrate of calmodulin-dependent kinases) has also been implicated[27,28]. But the difference in the localization of phosphorylating enzymes of these two proteins indicates that they have distinct roles in the transmitter release process. It may be that the regulatory role of B-50 in vesicle fusion is not limited to transmitter release, but extends to membrane-fusion processes during neurite outgrowth[29,30]. It remains to be investigated to what extent calmodulin binding[14] and modulation of phosphatidyl inositol 4-phosphate kinate activity[12,13]—putative properties of B-50—are also involved in controlling neurotransmitter release. □

Received 17 April; accepted 11 September 1989.

1. Aitgaier, C., Von Kügelgen, O. & Hertting, G. *Eur. J. Pharmacol.* **129,** 389–392 (1986).
2. Malenka, R. C., Ayoub, G. S. & Nicoll, R. A. *Brain Res.* **403,** 198–203 (1987).
3. Nichols, R. A., Haycock, J. W., Wang, J. K. T. & Greengard, P. *J. Neurochem.* **48,** 615–621 (1987).
4. Kaczmarek, L. K. *Trends Neurosci.* **10,** 30–34 (1987).
5. Malenka, R. C., Madison, D. V. & Nicoll, R. A. *Nature* **321,** 175–177 (1986).
6. Malinow, R., Madison, D. V. & Tsien, R. W. *Nature* **335,** 820–824 (1988).
7. Akers, R. F., Lovinger, D. M., Colley, P. A., Linden, D. J. & Routtenberg, A. *Science* **231,** 587–589 (1986).
8. Zwiers, H., Schotman, P. & Gispen, W. H. *J. Neurochem.* **34,** 1689–1699 (1980).
9. Alnyo, V. J., Zwiers, H. & Gispen, W. H. *J. Neurochem.* **41,** 649–653 (1983).
10. De Graan, P. N. E., Dekker, L. V., Oestreicher, A. B., Van der Voorn, L. & Gispen, W. H. *J. Neurochem.* **52,** 17–23 (1989).
11. Skene, J. H. P. *A. Rev. Neurosci.* **12,** 127–156 (1989).
12. Jolles, J. *et al. Nature* **286,** 623–625 (1980).
13. Gispen, W. H., Van Dongen, C. J., De Graan, P. N. E., Oestreicher, A. B. & Zwiers, H. in *Inositol and Phosphoinositides* (eds Bleasdale, J. E., Hauser, G. & Fichberg, J. 399–413 (Humana, Clifton, New Jersey 1985).
14. Andreasen, T. J., Luetje, C. W., Heideman, W. & Storm, D. R. *Biochemistry* **22,** 4615–4618 (1983).
15. Skene, J. H. P. & Willard, M. *J. Cell Biol.* **89,** 86–95 (1981).
16. Goslin, K., Schreyer, D. J., Skene, J. H. P. & Banker, G. *Nature* **336,** 672–674 (1988).
17. Lovinger, D. M. *et al. Brain Res.* **343,** 137–143 (1985).
18. Dekker, L. V., De Graan, P. N. E., Versteeg, D. H. G., Oestreicher, A. B. & Gispen, W. H. *J. Neurochem.* **52,** 24–30 (1989).
19. Howell, T. W. & Gomperts, B. D. *Biochim. biophys. Acta* **927,** 177–183 (1987).
20. Verhage, M., Besselsen, E., Lopes Da Silva, F. H. & Gispen, W. E. J. M. *J. Neurochem.* **51,** 1667–1674 (1988).
21. Gispen, W. H., Leunissen, J. L. M., Oestreicher, A. B., Verkleij, A. J. & Zwiers, H. *Brain Res.* **328,** 381–385 (1985).
22. Benowitz, L. I., Apostolides, P. J., Perrone-Bizzozero, N., Finklestein, S. P. & Zwiers, H. *J. Neurosci.* **8,** 339–352 (1988).
23. Schrama, L. H. *et al. Soc. Neurosci. Abstr.* **14,** 197.15 (1988).
24. Dolphin, A. C., Errington, M. L. & Bliss, T. V. P. *Nature* **297,** 496–498 (1989).
25. Aniksztejn, L., Roisin, M. P., Amsellem, R. & Ben-Ari, Y. *Neuroscience* **28,** 387–392 (1989).
26. Skene, J. H. P. & Virag, I. *J. Cell Biol.* **108,** 613–624 (1989).
27. Bähler, M. & Greengard, P. *Nature* **326,** 704–707 (1987).
28. Hirokawa, N., Sobue, K., Kanda, K., Harada, A. & Yorifuji, H. *J. Cell Biol.* **108,** 111–126 (1989).
29. van Hooff, C. O. M. *et al. J. Cell Biol.* **108,** 1115–1125 (1989).
30. Zuber, M. X., Goodman, D. W., Karns, L. R. & Fishman, M. C. *Science* **244,** 1193–1195 (1989).
31. De Langen, C. D. J., Hogenboom, F. & Mulder, A. H. *Eur. J. Pharmacol.* **60,** 79–89 (1979).
32. Bergmeyer, H. U. & Bernt, E. in *Methoden der Enzymatischen Analyse* (ed. Bergmeyer, H. U.) 533–538 (Verlag Chemie, Weinheim, 1970).
33. Oestreicher, A. B., van Dongen, C. J., Zwiers, H. & Gispen, W. H. *J. Neurochem.* **41,** 331–340 (1983).
34. Lowry, O. H., Rosebrough, N. J., Farr, A. L. & Randall, R. J. *J. biol. Chem.* **193,** 265–275 (1951).

ACKNOWLEDGEMENTS. We thank W.W.M. Pijnappel for experimental assistance, Dr W.J. Vaartjes for advise on the lactate dehydrogenase assay and E. Kluis and L. Claessens for preparing the manuscript. This work was supported by MEDICON.

Production of antibodies in transgenic plants

Andrew Hiatt, Robert Cafferkey & Katherine Bowdish

Department of Molecular Biology, The Research Institute of Scripps Clinic, 10666 North Torrey Pines Road, La Jolla, California 92037, USA

COMPLEMENTARY DNAs derived from a mouse hybridoma messenger RNA were used to transform tobacco leaf segments followed by regeneration of mature plants. Plants expressing single gamma or kappa immunoglobulin chains were crossed to yield progeny in which both chains were expressed simultaneously. A functional antibody accumulated to 1.3% of total leaf protein in plants expressing full-length cDNAs containing leader sequences. Specific binding of the antigen recognized by these antibodies was similar to the hybridoma-derived antibody. Transformants having γ- or κ-chain cDNAs without leader sequences gave poor expression of the proteins. The increased abundance of both γ- and κ-chains in transformants expressing assembled gamma–kappa complexes was not reflected in increased mRNA levels. The results demonstrate that production of immunoglobulins and assembly of functional antibodies occurs very efficiently in tobacco. Assembly of subunits by sexual cross might be a generally applicable method for expression of heterologous multimers in plants.

The source of immunoglobulin mRNAs was a hybridoma cell line expressing a catalytic IgG_1 antibody (6D4) which binds a low molecular weight phosphonate ester (P3) and catalyses the hydrolysis of certain carboxylic esters. Constructs used for immunoglobulin expression in plants consisted of coding-length cDNAs of the 6D4 γ- or κ-chain with or without their leader sequences. These cDNAs were modified to contain terminal *Eco*R1 restriction enzyme digestion sites and were ligated into the constitutive plant expression vector pMON530 (ref. 2) to form pHi101 (kappa, no leader), pHi102 (kappa, leader), pHi201 (gamma, no leader) and pHi202 (gamma, leader). We transformed tobacco plants using Agrobacterium containing each of these four plasmids[3] and screened leaf extracts from regenerated transformants for the presence of immunoglobulin heavy or light chains by enzyme-linked immunosorbent assay (ELISA)[4]. Transformants expressing individual immunoglobulin chains were then sexually crossed to produce progeny expressing both chains. The results of the ELISA revealed high levels of kappa and gamma chains accumulating in individual plants containing DNA from both pHi102 and pHi202 (Table 1; Fig. 2*a*). We verified the expression of both heavy and light chains by western blotting (Fig. 1). From the ELISAs, we judged that virtually all the γ- and κ-chains in these plants were assembled into gamma–kappa complexes (Table 1). Western blots provided additional evidence for assembled antibodies in that, under non-reducing conditions, most of the immunoreactive γ- and κ-chains aggregated at a high molecular weight (Fig. 1).

The binding specificity of the assembled gamma–kappa complexes was studied in ELISAs in which a P3–bovine serum albumin conjugate was used as antigen. The antigen binding by antibody derived from plants was equivalent to antigen binding by the 6D4 hybridoma antibody. Incubation of plant extracts or the purified 6D4 antibody with 50 μmol l^{-1} P3 for 3 h at 25 °C before addition to the ELISA eliminated antibody binding to the P3–BSA conjugate, demonstrating that binding was specific for the P3 hapten. Half-maximal inhibition occurred with 10 μmol l^{-1} free P3 for both hybridoma and plant-derived antibodies.

Transformants derived from the leaderless constructs pHi101 and pHi201 contained very low levels of κ- and γ-chains respectively, but Southern and northern blots (Fig. 2) demonstrated the presence of transforming DNA and immunoglobulin transcripts. None of the plants expressing leaderless

immunoglobulin chains contained assembled gamma-kappa complexes (Table 1).

The increased recovery of immunoglobulin epitopes from transformants expressing full-length cDNAs was not reflected in increased mRNA transcript levels. Northern blots (Fig. 2*b*) comparing pHi201 and pHi202 transformants, for example, revealed nearly equivalent levels of heavy-chain transcripts, although ELISAs indicated a 40-fold increase in accumulation of heavy-chain protein in the pHi202 transformant. Likewise, immunoglobulin mRNA levels in a plant producing large amounts of assembled antibodies were not significantly different from the parental plants that accumulated low levels of immunoglobulin chains (Fig. 2*b*).

Our results show that individual cDNAs for immunoglobulin κ- and γ-chains can be efficiently expressed in tobacco to form functional antibodies. Assembly of immunoglobulin chains by sexual cross in plants represents a useful alternative to the expression by a single vector of both gamma and kappa cDNAs as in yeast or bacteria[5-7], or double transformation with vectors containing individual cDNAs[8,9]. Potentially, this method is applicable to the assembly of oligomers other than antibodies. The characterization of antibodies produced in plants (glycosylation, processing of leader sequences, cytolocalization and turnover) will be described in a later paper.

In B lymphocytes, immunoglobulin processing and assembly occurs in the endoplasmic reticulum/Golgi in a process that may be promoted by heavy-chain binding proteins present in the endoplasmic reticulum[10,11]. Plant cells may also have a system for multimer assembly in their endoplasmic reticulum/Golgi that can recognize immunoglobulin chains. Alternatively, assembly may occur spontaneously, given sufficient levels of each chain in the appropriate cellular compartment. Our results demonstrate that plants require a signal sequence for efficient assembly of γ- and κ-subunits. The presence of the mouse leader sequence clearly augments the accumulation of individual chains. This might be the result of an enhanced translation of the immunoglobulin messengers or an increased stability of each protein as a result of subcellular sequestering or secretion. The yield of each chain is increased in plants expressing both gamma and kappa, indicating that assembly of the gamma-kappa complex might enhance stability.

TABLE 1 Expression and assembly of immunoglobulin gamma and kappa chains in tobacco

Accumulation of γ- or κ-chains in transformed plants*

γNL	γL	γL(κL)	γNL(κNL)
30 ± 16 (60)	1,412 ± 270 (2,400)	3,330 ± 2,000 (12,800)	32 ± 26 (60)
κNL	**κL**	**κL(γL)**	**κNL(γNL)**
1.4 ± 1.2 (3.5)	56 ± 5 (80)	3,700 ± 2,300 (12,800)	6.6 ± 6 (20)

Distribution and assembly in crosses†

	γ only	κ only	γκ	Null
κNL × γNL	4	6	3 (0% assembly)	5
κL × γL	3	10	11 (95 ± 16% assembly)	4

* Accumulation of individual gamma and kappa chains (in ng per mg total protein) was estimated by ELISA[4]. Microtitre wells were coated with a goat anti-mouse heavy or light chain-specific IgG (Fisher) in 150 mM NaCl, 20 mM Tris-HCl, pH 8.0 (TBS), followed by blocking with 5% non-fat dry milk in TBS. Plant leaves were homogenized in a mortar and pestle at 4 °C after removal of the midvein. To the supernatant a quarter volume of 5 × TBS was added, and 50 μl of 1 in 2 serial dilutions were added to each microtitre well. After 18 h at 4 °C, microtitre wells were washed with distilled water at room temperature. Bound γ- or κ-chains were reacted with goat anti-mouse heavy or light chain-specific antibodies conjugated to horseradish peroxidase for 2 h at 37 °C in TBS, and detected according to the manufacturer's instructions. Control microtitre wells contained extracts from plants transformed with pMON530 vector. Values given as mean (± s.d.) are derived from at least two determinations per plant and do not include transformants producing no detectable γ- or κ-chain. At least nine plants were assayed in each category. All values are given as ng per mg of total protein in the extract and are derived from the quantity of purified 6D4 antibody required to given an equivalent colour development in ELISA. Total protein in the extract was determined by the Bio-Rad Coomassie assay. Complementary DNAs containing no leader sequences are referred to as γNL and κNL; γL and κL refer to cDNAs with leader sequences; γ(κ) refers to gamma chains in a plant that also expresses κ-chains, and vice versa. Numbers in parentheses are values for plants with the highest levels of accumulation.

† The number of plants expressing γ- or κ-chains among the progeny of a sexual cross. The ELISA for assembly used horseradish peroxidase-conjugated anti-κ-chain-specific antibodies to detect antigen bound to microtitre wells coated with unlabelled anti-γ-chain-specific antibodies, and vice versa. Values derived from these assays were used to calculate the per cent of assembly by comparison with the purified 6D4 antibody. This was determined at least three times for each γκ plant. The per cent assembly is expressed in parentheses as the mean ± s.d.

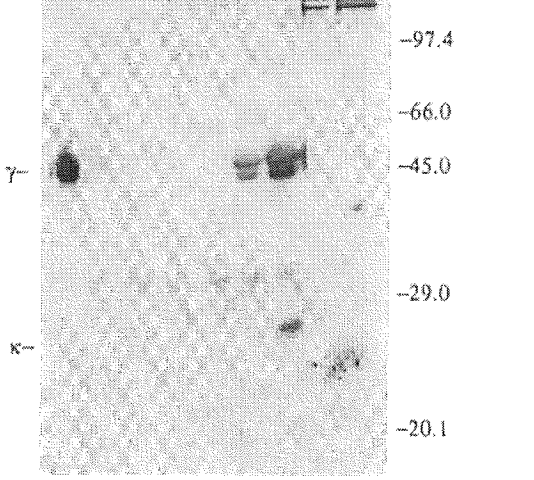

FIG. 1 Western blot of leaf proteins from transgenic tobacco plants expressing immunoglobulin chains. Leaf segments (1 g) from mature plants were homogenized in a mortar and pestle with 1 ml 0.05 M Tris-HCl, pH 7.5, 1 mM phenylmethanesulphonyl fluoride. Extracts were boiled in 4 M urea, 1% SDS, with or without 2 mM dithiothreitol (DTT) as indicated, for 3 min. SDS-PAGE in 10% acrylamide[16] and blotting of the proteins to nitrocellulose[17] were performed as described. Blots were preincubated for 6 h at 4 °C in 20 mM Tris-HCl, pH 8.0, 150 mM NaCl, 0.01% Tween 20 (TBST) containing 5% BSA, and 0.5% non-fat dried milk before the addition of antibodies. A biotinylated goat anti-mouse whole IgG antibody (Cappel), diluted 1:500 in TBST was used to probe the blots at 4 °C for 24 h. A variety of commercially available antibodies (anti-mouse IgGs) were used in other experiments with similar results. Antibody binding was visualized after binding of streptavidin-conjugated alkaline phosphatase (25 °C, for 2 h) by incubation in 300 μg ml^{-1} nitroblue tetrazolium and 150 μg ml^{-1} 5-bromo-4-chloro-3-indolyl phosphate. In lanes 1–7, 40 μl of each extract containing DTT; lanes 8 and 9, 40 μl extract without DTT. Lane 1, 100 ng purified antibody from the 6D4 hybridoma; lane 2, 15 μg wild-type plant-extract protein; lane 3, 15 μg protein from a plant transformed with truncated κ-chain cDNA (pHi101) containing no leader sequence; lane 4, 15 μg from plant transformed with truncated γ-chain cDNA (pHi201); lane 5, 15 μg from a full-length kappa cDNA transformant (pHi102); lane 6, 15 μg from a full-length γ-chain cDNA transformant (pHi202); lane 7, 15 μg from an F1 plant derived from the cross between a kappa and a gamma producer; lane 8, 100 ng 6D4 antibody (no DTT); lane 9, same as lane 7, except no DTT. Gamma and kappa on the left refer to the positions of the 6D4 heavy and light chains; positions of molecular weight (given in thousands) markers are shown on the right. By ELISA, extracts in lanes 3–5 contained very low levels of κ- or γ-chains (<0.008% of total protein, Table 1), whereas extracts in lanes 6, 7 and 9 contained 0.24, 1.3 and 1.3% immunoglobulin respectively.

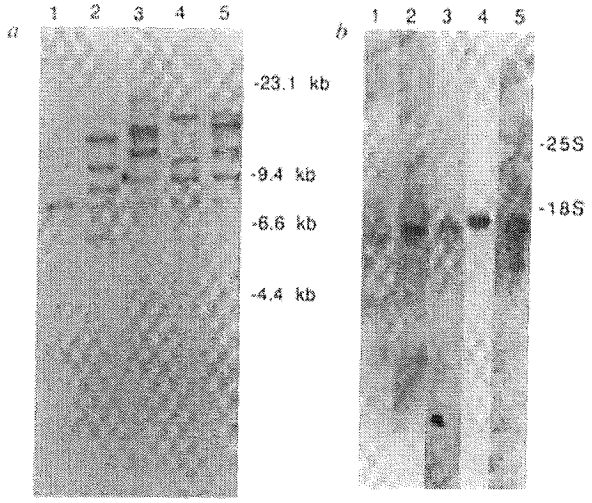

FIG. 2 Southern and northern blots of leaf DNA and RNA from transgenic plants expressing immunoglobulin cDNAs. *a*, DNA was extracted from 1 g mature leaf tissue after freezing the fresh segments in liquid N_2. Homogenization into urea mix[18] was in a mortar and pestle. The homogenate was extracted with phenol:$CHCl_3$ (1:1) and the nucleic acids precipitated by addition of one volume of isopropyl alcohol. The resuspended DNA (20 μg each) was cut with *Hind*III and Southern-blotted as described[19]. The probe used for both Southern and northern blots was ^{32}P-labelled pMON530 plasmid[2] containing either a kappa cDNA or a gamma cDNA. Both cDNAs were used in the hybridization shown. Lane 1, DNA from a transformant expressing a light-chain cDNA without a leader sequence (pHi101); lane 2, DNA from a heavy-chain cDNA transformant, no leader (pHi201); lane 3, DNA from a transformant expressing full-length light chain with leader (pHi102); lane 4, DNA from a transformant expressing heavy chain with leader (pHi202); lane 5, DNA from an F_1 plant derived from a cross between plants expressing full-length gamma or kappa cDNAs (pHi102 × pHi202). *b*, Extraction of RNA from 1 g fresh leaf tissue was by homogenization in 10 ml 0.1 M Tris-HCl, pH 9.0, and 10 ml phenol saturated with this buffer, using a Polytron at high speed. Nucleic acids were precipitated by addition of one tenth volume 3.0 M sodium acetate, pH 5.0, and 1.5 volumes isopropyl alcohol. Resuspended RNA was electrophoresed in gels containing formaldehyde and northern blotted onto nylon membranes (Amersham) as described[19]. Lane 1, RNA from a transformant expressing a light-chain cDNA without a leader sequence (pHi101); lane 2, RNA from a heavy-chain cDNA transformant, no leader (pHi201); lane 3, RNA from a transformant expressing full-length light chain with leader (pHi102); lane 4, RNA from a transformant expressing heavy chain with leader (pHi202); lane 5, RNA from an F_1 plant derived from a cross between plant expressing full-length gamma or kappa cDNAs (pHi102 × pHi202). Total RNA (20 μg) was loaded in each lane. Lanes from separate hybridizations were aligned with respect to the 18S (1,900 base pairs) and 25S (3,700 base pairs) ribosomal RNA bands on the blots, detected by methylene-blue staining.

Expression of functional antibodies from transcripts that do not contain signal sequences may require modifications to yield alternative antigen-binding structures (such as single-chain antigen-binding proteins[6,7]) that do not need to be assembled. Thus binding of constituents of metabolic pathways involved in morphogenesis, stress responses or plant–pathogen interactions could be used to further our understanding of these processes in a way analogous to the blocking by microinjected antibodies of specific protein functions in mammalian cells[12,13].

As large macromolecules such as protein multimers do not pass through plant cell walls[14,15], the binding by antibodies of small organic molecules (toxins, herbicides, plant hormones, organic chelates, for example) that are permeable to the cell wall might result in the net uptake and retention of these molecules in the plant. Accumulation of functioning antibodies may provide new options for the recovery of an array of environmental contaminants, as well as other biologically significant organics. Catalytic processing of small molecules within cell wall boundaries by antibodies may also become a generalized strategy for the elimination or modification of permeable organic compounds and could introduce new catalytic properties into existing metabolic pathways. □

Received 21 July; accepted 22 September 1989.

1. Tramontano, A., Janda, K. D. & Lerner, R. A. *Science* **234**, 1566–1570 (1987).
2. Rogers, S. G., Klee, H. J., Horsch, R. B. & Fraley, R. T. *Meth. Enzym.* **153**, 253–277 (1987).
3. Horsch, R. B. *et al. Science* **227**, 1229–1231 (1985).
4. Engvall, E. & Perlmann, P. *J. Immun.* **109**, 129–135 (1972).
5. Carlson, J. R. *Mol. cell. Biol.* **8**, 2638–2646 (1985).
6. Huston, J. S. *et al. Proc. natn. Acad. Sci. U.S.A.* **85**, 5879–5883 (1988).
7. Bird, R. E. *et al. Science* **242**, 423–426 (1988).
8. Wood, C. R. *et al. Nature* **314**, 446–449 (1985).
9. Horwitz, A. H., Chang, C. P., Better, M., Hellstrom, K. E. & Robinson, R. R. *Proc. natn. Acad. Sci. U.S.A.* **85**, 8678–8682 (1988).
10. Tartakoff, A. & Vassalli, P. *J. Cell Biol.* **83**, 284–299 (1979).
11. Munro, S. & Pelham, H. R. B. *Cell* **46**, 291–300 (1986).
12. Lamb, N. J. C. *et al. J. Cell Biol.* **106**, 1955–1971 (1988).
13. Rapaport, R. T., Venatha, R. J., Ziff, E. B., Lamb, N. J. & Feramisco, J. R. *Mol. cell. Biol.* **8**, 1670–1676 (1988).
14. Milburn, J. A. *Water Flow in Plants* Longman, London, 1979).
15. Carpita, N., Sabularse, D., Montezinos, D. & Delmer, D. P. *Science* **205**, 1144–1147 (1979).
16. Chua, N-H. *Meth. Enzym.* **69**, 434–446 (1980).
17. Harlow, E. & Lane, D. *Antibodies: A Laboratory Manual* (Cold Spring Harbor Laboratory, New York 1988).
18. Shure, M., Wessler, S. & Fedoroff, N. *Cell* **35**, 225–233 (1983).
19. Maniatis, T., Fritsch, E. F. & Sambrook, J. *Molecular Cloning, A Laboratory Manual* (Cold Spring Harbor Laboratory, New York 1982).

ACKNOWLEDGEMENTS. We thank Andrew Gelman for technical assistance, and Drs Mich. Hein, Richard Lerner, Richard Fair and Stephen Mayfield for discussion during the preparation of the manuscript.

Leu-8/TQ1 is the human equivalent of the Mel-14 lymph node homing receptor

David Camerini, Stephen P. James*, Ivan Stamenkovic† & Brian Seed

Departments of Molecular Biology, Massachusetts General Hospital, Genetics and † Pathology, Harvard Medical School, Boston, Massachusetts 02114, USA
* Section on Mucosal Immunity, Laboratory of Clinical Investigation, National Institute of Allergy and Infectious Diseases, Bethesda, Maryland 20892, USA

THE human pan-leukocyte antigen Leu-8 has attracted wide interest because its presence or absence identifies suppressor-inducer and helper-inducer CD4$^+$ T-lymphocyte subsets respectively. We report here that Leu-8 is the human homologue of the mouse Mel-14 homing receptor, a molecule that promotes the initial adhesion of blood-borne lymphocytes to the specialized post-capillary endothelium of peripheral lymph nodes. We also show that Leu-8 can adopt both conventional and phospholipid anchored forms, a finding that may have relevance in the context of antigen shedding following activation or homing. The assignment of lymphocytes to different functional classes based on lymph node homing potential may represent a more general association between lymphocyte function and tissue distribution.

Two complementary DNA clones encoding Leu-8 determinants were isolated from a human T-cell library by methods previously described[1,2]. DNA sequence analysis showed that the longer insert of the two contains 2,350 residues, whereas the shorter lacks 436 internal residues but is otherwise identical (Fig. 1). The predicted polypeptide sequences were found to diverge at their C-termini.

The protein encoded by the larger insert bears a strongly hydrophobic putative membrane spanning domain near its C terminus, followed by several positively charged residues resembling a cytoplasmic anchor sequence. The protein is closely related to the recently described murine Mel-14 homing receptor[3,4] (Fig. 1) and the corresponding cDNA sequence shares

The Internal Propeptide of the Ricin Precursor Carries a Sequence-Specific Determinant for Vacuolar Sorting[1]

Lorenzo Frigerio*, Nicholas A. Jolliffe, Alessandra Di Cola, Doramys Hernández Felipe, Nadine Paris, Jean-Marc Neuhaus, J. Michael Lord, Aldo Ceriotti, and Lynne M. Roberts

Department of Biological Sciences, University of Warwick, Coventry CV4 7AL, United Kingdom (L.F., N.A.J., A.D.C., J.M.L., L.M.R.); Laboratorie de Biochimie, Université de Neuchâtel, rue Émile-Argand 9, CH–2007 Neuchâtel 7, Switzerland (D.H.F., N.P., J.-M.N.); and Istituto Biosintesi Vegetali, Consiglio Nazionale delle Ricerche, via Bassini 15, 20133 Milano, Italy (A.C.)

Ricin is a heterodimeric toxin that accumulates in the storage vacuoles of castor bean (*Ricinus communis*) endosperm. Proricin is synthesized as a single polypeptide precursor comprising the catalytic A chain and the Gal-binding B chain joined by a 12-amino acid linker propeptide. Upon arrival in the vacuole, the linker is removed. Here, we replicate these events in transfected tobacco (*Nicotiana tabacum*) leaf protoplasts. We show that the internal linker propeptide is responsible for vacuolar sorting and is sufficient to redirect the ricin heterodimer to the vacuole when fused to the A or the B chain. This internal peptide can also target two different secretory protein reporters to the vacuole. Moreover, mutation of the isoleucine residue within an NPIR-like motif of the propeptide affects vacuolar sorting in proricin and in the reconstituted A-B heterodimer. This is the first reported example of a sequence-specific vacuolar sorting signal located within an internal propeptide.

Soluble proteins targeted to plant vacuoles need specific signals to reach their destination. These signals have been recently divided in three categories: sequence-specific vacuolar sorting signals (ssVSS), C-terminal signals (ctVSS), and physical structure signals (psVSS; Matsuoka and Neuhaus, 1999; Vitale and Raikhel, 1999). ssVSS are predominantly located at the N terminus and present an NPIR-like motif, which is necessary for sorting of sporamin (Matsuoka and Nakamura, 1991). The NPIR-containing sporamin propeptide is sufficient to target a secreted reporter protein to the vacuole (Matsuoka et al., 1995). Putative sorting receptors that bind to NPIR-containing peptides have been identified in pea (Kirsch et al., 1994), Arabidopsis (Ahmed et al., 1997, 2000), and pumpkin (Shimada et al., 1997). The presence of the isoleucine residue in NPIR is essential for sorting and in vitro binding to the putative receptors, suggesting that its large hydrophobic side chain is crucially involved in the interaction (Matsuoka and Nakamura, 1999; Cao et al., 2000).

ctVSS are extremely variable in size and amino acid composition and although no consensus sequence has been identified, a common requirement is the presence of a C-terminally exposed hydrophobic amino acid patch (Matsuoka and Neuhaus, 1999; Vitale and Raikhel, 1999). The third class of signals is rather ill defined at present. Internal folded domains of proteins have been shown to be necessary for sorting, for example in the case of phytohemagglutinin (von Schaewen and Chrispeels, 1993) and in the case of the saposin-like insert of barley phytepsin (Kervinen et al., 1999), but they have not yet been characterized. The fact that these domains are part of the mature protein has led to the hypothesis that interaction with a sorting receptor requires particular structural features in the native domain (Matsuoka and Neuhaus, 1999).

In the present work we report characterization of the internal sorting signal of proricin, which is processed upon vacuolar delivery. We also show that this internally cleaved propeptide is necessary and sufficient for vacuolar sorting and that it is functionally similar to a normally N-terminal ssVSS.

Ricin is a type II (heterodimeric) ribosome-inactivating protein (RIP) that accumulates in the castor bean (*Ricinus communis*) endosperm. Ricin is synthesized as a single precursor protein (proricin) where the catalytically active A chain (RTA) is joined to the sugar-binding B chain (RTB) by a 12-amino acid "linker" peptide (Lamb et al., 1985). Preproricin is translocated into the endoplasmic reticulum (ER) lumen via a 35-residue presequence, the first 26 residues of which represent an ER signal peptide (Ferrini et al., 1995). The remaining nine residues, absent from mature RTA, must therefore form an N-terminal propeptide (Lamb et al., 1985). Within the ER, proricin is glycosylated and disulfide bonded within RTB and between the RTA and RTB regions. In castor bean en-

[1] This work was supported in part by the European Union (grant no. CHRX-CT94–0590), by the Biotechnology and Biological Science Research Council (grant no. 88/C08612), by the British Council/Ministero dell'Universita'e della Ricerca Scientifica e Tecnologica (grant no. ROM/889/99/10), and by the Swiss National Science Foundation (grant no. 31–46926.96).

* Corresponding author; e-mail l.frigerio@warwick.ac.uk; fax 44–2476–523701.

dosperm cells, proricin is then transported via the Golgi complex to the periphery of precursor accumulating vesicles (PAC; Hara-Nishimura et al., 1998), and eventually to protein storage vacuoles. There the N-terminal and the linker propeptides are proteolytically cleaved, releasing the mature, disulfide-linked heterodimeric toxin (Butterworth and Lord, 1983; Lord, 1985; Hara-Nishimura et al., 1995).

We have recently demonstrated that it is possible to transiently express the cytotoxic proricin in tobacco (*Nicotiana tabacum*) leaf mesophyll protoplasts and that the intracellular transport events normally occurring in castor bean are faithfully reproduced in the heterologous system (Frigerio et al., 1998b). That is, preproricin reaches the vacuole through the Golgi complex and is processed to its mature form. When we fused the single A and B chains, engineered to lack the linker peptide, to signal peptides and coexpressed them in protoplasts, RTA and RTB associated very rapidly to form the disulfide-linked ricin heterodimer within the ER lumen. However, unlike proricin, the heterodimer was quantitatively secreted into the extracellular medium (Frigerio et al., 1998b). This led us to speculate whether the presence of the internal linker peptide could be necessary for vacuolar sorting. Here we report that this is the case, and we characterize the linker as a ssVSS of the sort more typically found at the N terminus of vacuolar proproteins.

RESULTS

Preproricin Reaches the Vacuole via Vesicular Transport in Tobacco Protoplasts

We characterized the intracellular fate of preproricin in tobacco protoplasts. The preproricin sequence (ppricin) was placed downstream of the cauliflower mosaic virus (CaMV) 35S promoter (Fig. 1) and transiently expressed in tobacco protoplasts. Protoplasts transfected with the ppricin construct were subjected to pulse-chase analysis and ricin polypeptides detected by immunoprecipitation with anti-RTA antiserum, followed by 15% (w/v) SDS-PAGE and fluorography (Fig. 2). At the end of the pulse, an immunoreactive polypeptide of the size expected for preproricin was detected (open arrowhead, Fig. 2, lane 1). This polypeptide disappeared with time and was eventually converted into two polypeptides of the sizes expected for mature glycosylated RTA and RTB (32 and 34 kD, respectively, lanes 2 and 3). Such proteolytic processing normally occurs within the storage protein vacuoles of castor bean endosperm cells (Harley and Lord, 1985; Hara-Nishimura et al., 1995). The appearance of processed subunits is therefore indicative of the arrival of proricin within vacuolar compartments. By non-reducing PAGE analysis we have previously shown that such processed polypeptides are linked by a disulfide bond and are stored as heterodimeric ricin (Frigerio et al., 1998b).

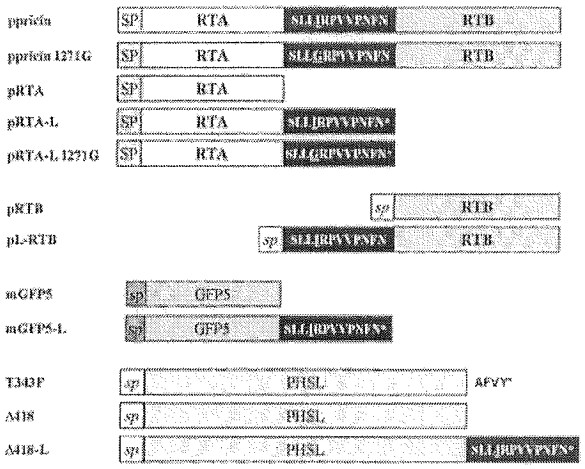

Figure 1. Schematic diagram of the constructs used in this work. All coding sequences were under the control of the CaMV 35S promoter. SP, Preproricin signal peptide; sp, prephaseolin signal peptide; sp, Arabidopsis basic chitinase signal peptide.

Because RTA and RTB are covalently linked by a disulfide bridge, anti-RTA antiserum immunoselects the RTA-RTB heterodimer, which is then reduced into its two components upon reducing SDS-PAGE analysis. Treatment of cells with the fungal metabolite brefeldin A (BFA) inhibited the formation of mature polypeptides and led to the accumulation of intact proricin (Fig. 2, lanes 4–6). BFA has been previously shown to inhibit Golgi-mediated transport to vacuoles in plant cells (Gomez and Chrispeels, 1993; Pedrazzini et al., 1997). This suggests that preproricin is being targeted to its site of processing via Golgi-mediated transport. No extracellular secretion of preproricin or mature ricin was detected (Fig. 1, lanes 7–12). Overall, therefore, the sequence of events observed here is consistent to that occurring in the endosperm cells of castor bean seeds.

The Presence of the Linker Peptide Causes Vacuolar Sorting Even When It Is Not in Peptide Continuity with Both Ricin Subunits

So far we have shown that preproricin is transported via a Golgi-mediated trafficking pathway to vacuoles in a BFA-sensitive fashion. Previous work suggested that the vacuolar sorting signal might lay within the 12-aminoacyl residue linker that is localized between the A and B chains of proricin (Frigerio et al., 1998b). We next tested whether peptide continuity of the subunits with the linker is required for functional sorting to vacuoles. We cotransfected protoplasts with RTA and RTB, or RTA-L and RTB, or RTA and L-RTB (Fig. 1), and then subjected the cells to pulse-chase followed by immunoprecipitation with anti-RTA antiserum. In this and other experiments (e.g. in Fig. 7B) the amount of radiolabeled RTB coprecipitated with RTA somehow increased

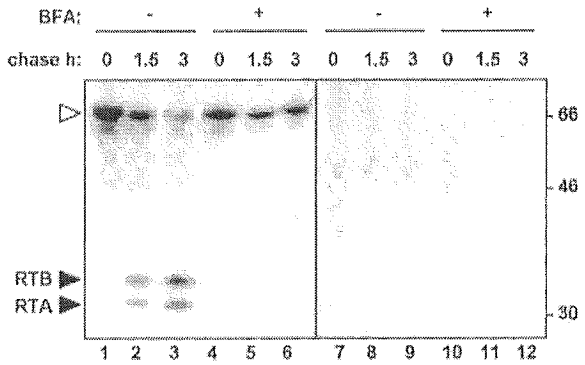

Figure 2. Transport of proricin to vacuoles is sensitive to BFA in tobacco leaf protoplasts. A, Protoplasts from tobacco leaves were transfected with the ppricin construct, pulse labeled for 1 h in the presence (+) or in the absence (-) of 10 μg mL^{-1} of BFA, and chased for the indicated periods of time. Cell homogenates (lanes 1–6) and incubation media (lanes 7–12) were subjected to immunoprecipitation with rabbit anti-RTA antiserum and analyzed by SDS-PAGE and fluorography. White arrowheads indicate the position of proricin and black arrowheads indicate mature RTA and RTB. Numbers at right indicate molecular mass markers in kilodaltons.

during the chase. The reason for this increase was not investigated, but it may be dependent on the kinetics of RTA-RTB assembly. As shown in Figure 3A, most of the ricin made by expressing pRTA and pRTB in the absence of the linker (Fig. 3A, lanes 1–3) was secreted after a 5-h chase period (lanes 4–6). During secretion there was a clear increase in the mobility of RTB, which may be due to oligosaccharide trimming (Lord, 1985). When the linker was appended to the C terminus of RTA (Fig. 3B, lanes 1–3), the ricin heterodimers were retained within the cells. The addition of the linker peptide to the C terminus of RTA caused an observable decrease in electrophoretic mobility at the 0-h chase (Fig. 3B, lane 1). During the chase (lanes 2 and 3), this polypeptide showed a faster mobility compatible with the removal of the linker and possible removal of the N-terminal propeptide (as mentioned above). Likewise, addition of the linker peptide to the N terminus of RTB (Fig. 3C, lanes 1–3) blocked secretion of the heterodimers (lanes 4–6). Moreover, RTA and RTB underwent processing during the chase (Fig. 3C, lanes 2 and 3).

To verify whether this processing was effectively occurring in vacuoles, we cotransfected cells with pRTA-L and pRTB or with pL-RTB and pRTA and subjected them to pulse labeling for 5 h. Vacuoles were then purified and the ricin polypeptides immunoselected with anti-RTA antiserum (Fig. 3D). In all cases the final mobilities of the two cotransfected subunits were indistinguishable from the mobilities of mature RTA and RTB generated from proricin (compare lane 1 with lanes 2 and 3). The mature subunits were recovered from within purified vacuoles (Fig. 3D, lanes 4–6). Thus, we conclude that the linker does not have to covalently bridge both subunits to direct ricin to the vacuole, where the linker is proteolytically removed.

The Linker Peptide Is Sufficient to Redirect Reporter Proteins to Vacuoles

The results shown so far demonstrate that the linker peptide is necessary for vacuolar sorting of ricin, but they do not allow us to conclude that the linker is also sufficient; other domains present on

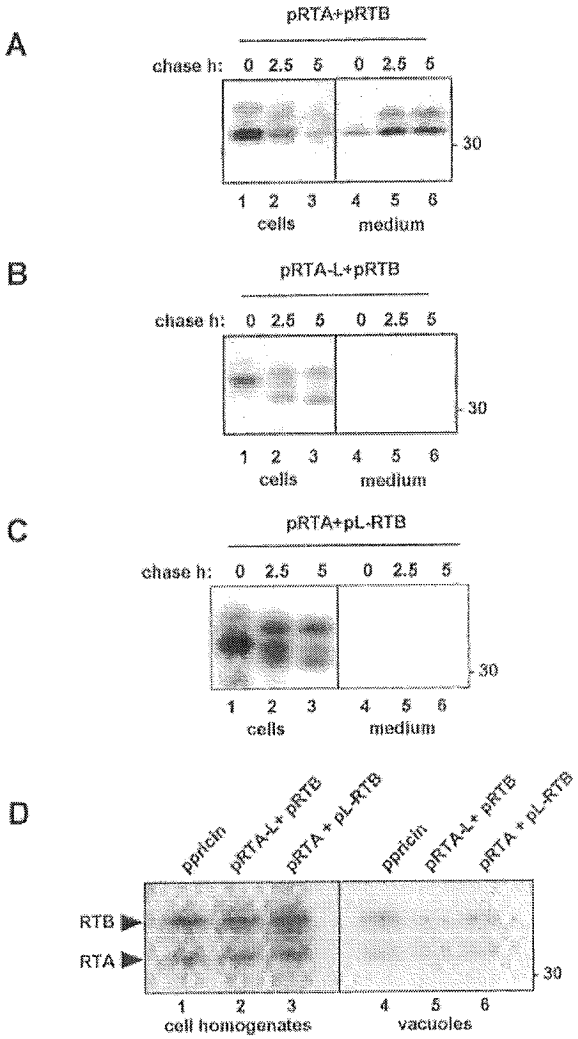

Figure 3. The presence of the linker peptide causes vacuolar sorting even when it is not in peptide continuity with both ricin subunits. A through C, Cells were transfected with the indicated constructs, pulse-labeled for 1 h, and chased for the indicated periods of time. Cell homogenates and incubation media were immunoprecipitated with anti-RTA antiserum and analyzed by SDS-PAGE and fluorography. Numbers at right indicate molecular mass markers in kilodaltons. D, Cells were transfected with the indicated constructs and subjected to pulse labeling for 5 h. Total cell homogenates or purified vacuoles were immunoprecipitated with anti-RTA antiserum and subjected to SDS-PAGE and fluorography.

RTA or RTB could contribute to a complete sorting signal. It is, therefore, necessary to examine whether the ricin linker peptide alone can redirect secreted reporter proteins to the vacuole. We, therefore, studied the fate of two reporter proteins: green fluorescent protein (GFP) and a secreted mutant of the storage protein phaseolin, Δ418 (Frigerio et al., 1998a). GFP has been recently used with success as a reporter for vacuolar targeting in vivo in tobacco protoplasts (Di Sansebastiano et al., 1998). We fused the 12-residue ricin linker to the C terminus of mGFP5 (a secretory version of GFP) to yield mGFP5-L (Fig. 1). As an expression system, we used protoplasts prepared from a suspension cell culture of Arabidopsis (Axelos et al., 1992). The advantage of these cells over tobacco leaf protoplasts is the homogeneity of the cell population, which seems to present only one type of large central vacuole, whereas tobacco protoplasts contain a mixed population of cells presenting different vacuolar structures that are, at present, difficult to characterize (Di Sansebastiano et al., 1998). In addition, leaf protoplasts contain chloroplasts whose autofluorescence interferes with the detection of GFP. We transfected Arabidopsis protoplasts with mGFP5 and mGFP5-L (Fig. 4A). Twenty-four hours after transfection, cells expressing mGFP5-L show strong fluorescence in their central vacuoles (Fig. 4A, note the absence of signal from the adjacent, nontransfected cells).

In a converse manner, cells expressing mGFP5 did not show any fluorescence with the same laser intensity settings (not shown), suggesting that the protein was secreted as expected (Boevink et al., 1999). We confirmed this evidence biochemically by transfecting tobacco protoplasts and subjecting them to pulse-chase, followed by immunoprecipitation with anti-GFP antiserum. Figure 4B shows that after 24 h, most mGFP5 is recovered in the extracellular medium (Fig. 4B, lanes 1–6). A proportion of mGFP5 molecules is still detectable intracellularly, and it has greater mobility than the extracellular GFP. However, tobacco protoplasts transfected with mGFP5-L do not secrete the reporter at all (Fig. 4B, lanes 7–12). Rather, GFP-L is converted with time to a faster migrating species, identical to the faster migrating form detectable intracellularly for mGFP5 (Fig. 4B, compare lanes 2 and 3 with lanes 8 and 9). This shows that addition of the linker peptide causes efficient intracellular retention of GFP. GFP undergoes intracellular proteolytic trimming at its C or N terminus, probably within vacuoles (Fig. 4A). The precise intracellular location and the sequence-specificity of this processing are at present unknown and their analysis is beyond the scope of this work.

In a further demonstration we showed that the ricin-linker peptide redirects a second reporter protein to vacuoles in tobacco protoplasts. In this case the linker was fused to phaseolin Δ418, a secretory

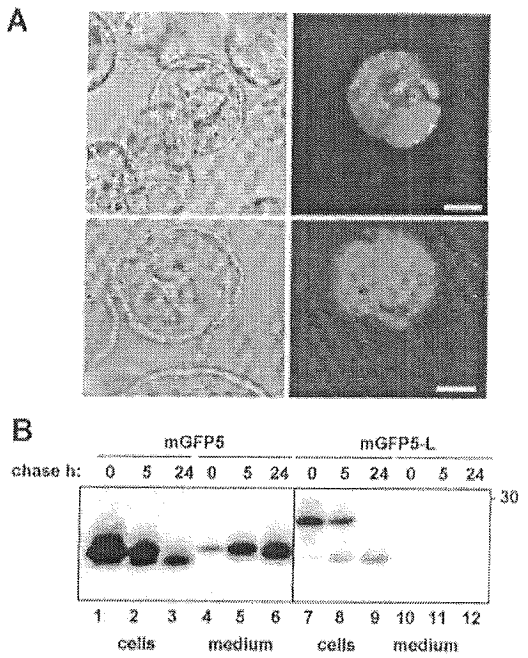

Figure 4. The linker peptide is sufficient to redirect GFP to the vacuole. A, Protoplasts from Arabidopsis suspension-cultured cells were transfected with mGFP5-L and analyzed by bright field (left) or fluorescence confocal microscopy (right) 24 h after transfection. Bar: 10 μm. B, Tobacco leaf protoplasts were transfected with mGFP5 or mGFP5-L, pulse labeled for 1 h, and chased for the indicated periods of time. Cell homogenates and incubation media were immunoprecipitated with anti-GFP antiserum and analyzed by SDS-PAGE and fluorography. The number at right indicates molecular mass marker in kilodaltons.

mutant of the vacuolar storage glycoprotein phaseolin (Frigerio et al., 1998a). Figure 5 shows that the 46-kD wild-type phaseolin (T343F; Pedrazzini et al., 1997) disappears during the chase period with the concomitant appearance of faster migrating polypeptides (Fig. 5, lane 2). These are known to represent proteolytic fragments of phaseolin that arise within heterologous storage vacuoles (Bagga et al., 1992; Pedrazzini et al., 1997). By contrast, a phaseolin mutant in which the four C-terminal amino acid residues (AFVY) were removed (phaseolin Δ418) did not generate such fragments internally, but was instead secreted into the extracellular medium (Frigerio et al., 1998a; Fig. 5, lanes 5, 6, 11, and 12). When this secretory phaseolin was tagged with the ricin linker to yield Δ418-L, it was efficiently retained within the cells (Fig. 5A, lanes 3, 4, 9, and 10). The appearance of proteolytic fragments, diagnostic of successful targeting to the vacuoles (Fig. 5, lane 4), confirms that the ricin linker is not only necessary for proricin vacuolar targeting, but also sufficient to redirect to the vacuole an otherwise secreted phaseolin mutant. A proportion of wild-type, as well as of Δ418-linker, phaseolin was also recovered in the medium (Fig. 5, lanes 7–10). We have previously demonstrated that this is due to

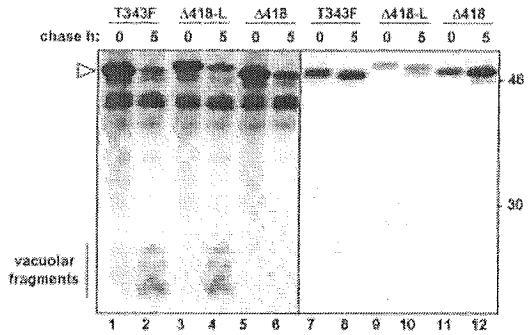

Figure 5. The linker peptide is sufficient to redirect phaseolin Δ418 to the vacuole. Tobacco leaf protoplasts were transfected with the indicated phaseolin constructs, pulse-labeled for 1 h, and chased for the indicated periods of time. Cell homogenates (lanes 1–6) and incubation media (lanes 7–12) were immunoprecipitated with anti-phaseolin antiserum and analyzed by SDS-PAGE and fluorography. The white arrowhead indicates intact phaseolin. Numbers at right indicate molecular mass markers in kilodaltons.

saturation of the vacuolar targeting machinery during the burst of protein synthesis following transient expression (Frigerio et al., 1998a). The amount of vacuolar fragments observed for wild-type and for Δ418-linker phaseolin is comparable (Fig. 5, compare fragments in lanes 2 and 4), suggesting that Δ418-linker phaseolin is also saturating the targeting machinery. The lower amount of secreted Δ418-linker compared with wild-type phaseolin (Fig. 5, compare lanes 7 and 10) likely reflects its lower overall expression levels (compare lane 1 with lane 3).

An Isoleucine Residue in the NPIR-Like Motif of the Linker Peptide Is Essential for Its Targeting Function

To determine whether the linker contains an ssVSS, or whether it is more typical of a ctVSS or psVSS we studied the primary sequence of the ricin-linker peptide. All type II RIPs contain a catalytic A subunit disulfide bonded to a Gal-specific lectin (B subunit). Therefore, we analyzed the primary sequence of the propeptides in several proricin-related proteins (Fig. 6): castor bean agglutinin, proabrin A from the abrin protein family of *Abrus precatorius* (Hung et al., 1993), two members of a group of type II RIPs isolated from elderberry (Van Damme et al., 1996), cinnamomin from *Cinnamomum camphora*, and a novel RIP recently isolated from *Polygonatum multiflorum* (Van Damme et al., 2000). Alignment of the linker peptides of these proproteins shows that an Ile residue, as well as the following Arg, are highly conserved. In ricin these residues exist within a sequence, LLIRP (Figs. 1 and 6), that resembles what is now regarded as the "canonic" consensus for an ssVSS. Matsuoka and Nakamura (1999) recently performed an extensive analysis of the sporamin ssVSS, NPIRL, which emphasized the importance of the Ile residue. The possibility that the Ile residue could be involved in the sorting of proricin was, therefore, investigated. We generated a mutant of preproricin where Ile 271 is changed to Gly (ppricin I271G, Fig. 1) and expressed I271G preproricin in tobacco protoplasts. Figure 7A clearly shows that the mutant proricin is secreted into the medium (Fig. 7A, lanes 10–12), in contrast to the wild-type toxin that remains intracellular and becomes processed to generate ricin subunits within the vacuoles (Fig. 7A, lanes 1–3). Thus, the Ile residue in the linker is essential for correct vacuolar targeting of proricin. A small proportion of secreted proricin I271G appeared to undergo fragmentation (Fig. 7A, lanes 11 and 12); this extracellular trimming could be due to hydrolases that are secreted by the protoplasts, as we have previously shown for a different reporter protein (Frigerio et al., 1998a).

When we introduced the same mutation into the linker fused to the C terminus of RTA (pRTA-L I271G), we observed secretion of the RTA-RTB heterodimer during the chase (Fig. 7B, lanes 7 and 8). Note that the secreted pRTA-L I271G did not undergo vacuolar processing and the presence of the linker on RTA caused it to comigrate with RTB. However, a proportion of the heterodimers was apparently vacuolar since we observed some intracellular processing (Fig. 7B, lane 4). Therefore, when the linker was positioned at the C terminus of RTA, mutation of the Ile did not completely abolish vacuolar sorting. This could mean that in this particular context, the two Leu residues adjacent to the mutated Ile are now playing a crucial role in receptor binding. In an alternate manner, it is possible that the proricin linker peptide is now being recognized by the vacu-

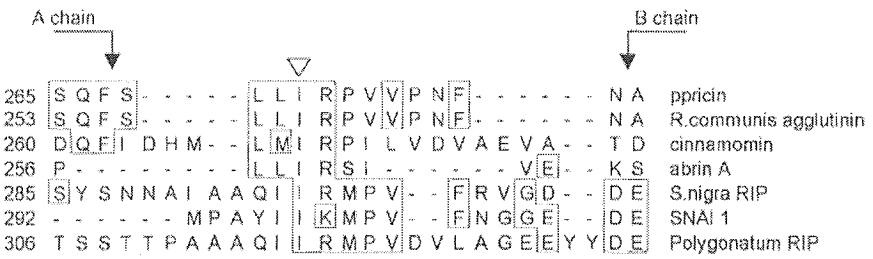

Figure 6. A conserved isoleucine residue in the linker peptides of proricin and proricin-related proteins. Amino acid sequence alignment was generated using the MegAlign program (DNAstar, Madison, WI). Identical amino acid residues are boxed. The conserved isoleucine residue is shown by an white arrowhead.

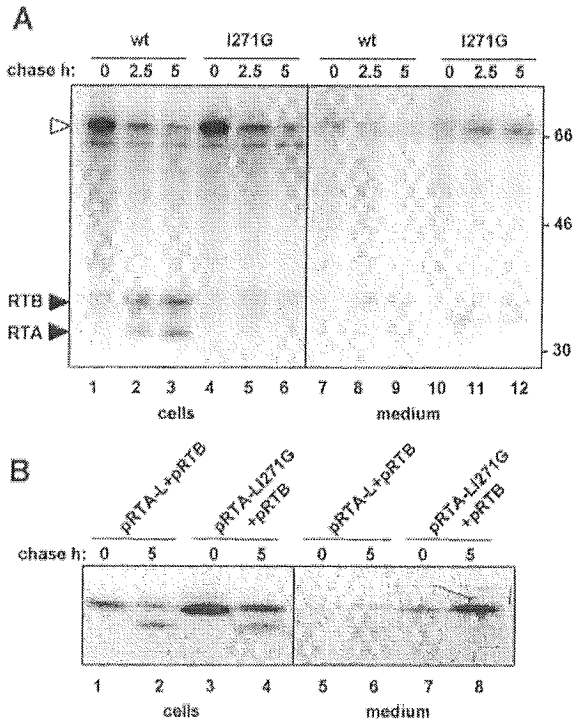

Figure 7. The isoleucine residue in the linker peptide is required for vacuolar sorting. A, Effect of the I271G on the intracellular fate of proricin. Cells were transfected with ppricin or ppricin I271G, pulse labeled for 1 h, and chased for the indicated periods of time. Cell homogenates and incubation media were immunoprecipitated with anti-RTA antiserum and analyzed by SDS-PAGE and fluorography. White arrowheads indicate the position of proricin and black arrowheads indicate mature RTA and RTB. Numbers at right indicate molecular mass markers in kilodaltons. B, Effect of the I271G mutation on the intracellular fate of the RTA-L/RTB heterodimer. Cells were transfected with the indicated constructs, pulse labeled for 1 h, and chased for the indicated periods of time. Cell homogenates and incubation media were immunoprecipitated with anti-RTA antiserum and analyzed by SDS-PAGE and fluorography.

olar sorting machinery as a signal of the C-terminal type (ctVSS).

DISCUSSION

An Internal, Processed Vacuolar Sorting Signal

We present evidence for a processed vacuolar-sorting signal that is located internally to a vacuolar proprotein. We have previously shown that the absence of the linker propeptide caused the mature ricin heterodimer to be secreted (Frigerio et al., 1998b). Here we show that the linker is able to redirect the dimer to the vacuole even when it is not in peptide continuity with RTA and RTB. This indicates that secretion of RTA-RTB dimers is not due to an indirect effect of the interruption in polypeptide continuity, but rather suggests that the linker itself contains vacuolar sorting information. The linker peptide proved sufficient to target two different reporter proteins to the vacuole. In the case of phaseolin Δ418, Figure 5 shows clearly that the linker can restore the efficiency of vacuolar sorting to wild-type levels. Moreover, the size of the vacuolar fragments is identical to those observed in the wild type, suggesting that as in the case of proricin and single ricin chain-linker fusions, the linker is ultimately removed. Likewise, when fused to GFP, the linker is efficient in abolishing secretion of the protein in tobacco protoplasts, and GFP-L accumulates in the large central vacuole of Arabidopsis protoplasts. A proportion of the secretory GFP (mGFP5) appears to be retained inside the cell and to undergo what resembles vacuolar processing (Fig. 4B, lanes 1–3); however, no fluorescence was detectable in Arabidopsis protoplasts expressing mGFP5. One possible explanation is that a proportion of mGFP5, which is not a natural secretory protein, may fold incorrectly (and therefore be incapable of fluorescing) to be eventually targeted to the vacuole by quality control mechanisms. We have recently demonstrated that when a hybrid immunoglobulin A/G (a secretory antibody) is expressed in transgenic tobacco, a large proportion of the molecules is delivered to the vacuole (Frigerio et al., 2000) instead of being secreted. Thus, the clear difference in GFP signal when protoplasts are transfected with mGFP5 or mGFP-L might be due to the accumulation of correctly folded protein in the vacuolar compartments only in the latter case.

The Isoleucine Is Essential for Targeting

The sequence of the linker peptide contains a motif (LLIRP) that resembles NPIRL. According to the consensus proposed by Matsuoka and Nakamura (1999) based on mutational analysis of the sporamin NPIRL sequence, the context for the Ile residue in the linker is by no means ideal, although it is worthy of note that the motif in the aleurain propeptide also contains Pro in position X4 (Holwerda et al., 1992). Nevertheless, exchanging the iso-Leu for Gly causes secretion of proricin, demonstrating that the Ile is critical for targeting, even in this theoretically not-ideal context. Our work has the advantage of demonstrating the sequence specificity feature of the proricin linker in vivo and in a native context. To our knowledge, this is the first example of a ssVSS located in an internal position.

It is interesting that when the I271G mutation was introduced into the C-terminal fusion of the linker with RTA, the phenotype was not one of complete secretion, and a proportion of the protein was still targeted to vacuoles. Similar results were obtained with the phaseolin-linker fusion (data not shown). One possible explanation is that the two Leu residues that are present immediately before I271 could, in the absence of the native proricin structural context, become exposed and substitute the Ile in binding to a

sorting receptor. Another possibility is that the linker peptide, when present at the C terminus of the protein, behaves partially as a ctVSS. This would not be surprising, as a similar phenotype was previously observed when the sporamin propeptide containing the corresponding I to G mutation was appended to the C terminus of sporamin (Koide et al., 1999).

Implications for Trafficking

We present evidence for a ssVSS that resides internally to a proprotein destined to storage vacuoles. NPIR-like motifs have been shown in vitro to be ligands for the putative sorting receptor BP-80/AtELP. The ssVSS-BP-80 interaction is believed to sort proteins into clathrin-coated vesicles for transport to the lytic vacuole via the pre-vacuolar compartment (Vitale and Raikhel, 1999). Proteins destined to the storage vacuole are believed to enter dense vesicles at the trans-Golgi; these vesicles do not contain BP-80 (Hinz et al., 1999) and this transport pathway appears to be more sensitive to treatment with wortmannin in tobacco bright yellow 2 cells (Matsuoka and Neuhaus, 1999), although it is not clear at present whether the dense vesicle pathway and the wortmannin-sensitive pathway coincide. The proricin linker peptide has the features of a potential BP-80 ligand, but ricin is a vacuolar storage protein. How do we interpret these apparently conflicting findings?

Hara-Nishimura and coworkers (1998) recently provided evidence that in pumpkin and castor bean endosperm, storage 2S albumins travel from the ER to the storage vacuole in large PAC. Terminally glycosylated storage proteins are found at the periphery of the PAC around the 2S albumin core. The authors detected these glycoproteins, which are believed to include ricin and castor bean agglutinin, using an antiserum raised against complex glycans (Hara-Nishimura et al., 1998). This is also compatible with the direct labeling of ricin subunits with tritiated Fuc in cell fractions corresponding to the Golgi apparatus (Lord, 1985). Together, this evidence suggests that these proteins have traveled through the Golgi complex where glycan processing occurs, before joining the PACs. Nothing is known about the mechanisms that sort such glycoproteins from the trans-Golgi to the periphery of the PAC. Nevertheless, it would be plausible to postulate the existence of a sorting receptor with similar specificities to those of BP-80 that captures glycoproteins at the trans-Golgi level and sorts them into the PAC, rather than into clathrin-coated vesicles. We speculate that proricin could be recognized by a BP-80-like receptor for sorting to PAC. In pumpkin seeds the PAC themselves have been shown to contain two proteins, PV72 and PV82, functionally similar to BP-80 (Shimada et al., 1997), which might be the endogenous receptors for 2S albumins. In a similar manner, proteins presenting a high degree of homology to the BP-80 lumenal, ligand-binding domain have recently been identified in dark intrinsic protein bodies, the likely precursors to the protein storage vacuole crystalloid in root tip cells and developing seeds (Jiang et al., 2000). Dark intrinsic protein bodies contain proteins whose glycans have undergone modification in the Golgi and could represent a form of multivesicular body that is functionally similar to the PAC (Jiang et al., 2000). Since it is well established that BP-80 orthologs can bind ssVSS regardless of their position in the polypeptide (Kirsch et al., 1996; Saalbach et al., 1996; Matsuoka and Neuhaus, 1999; Matsuoka, 2000), the internal location of the proricin ssVSS would not preclude it from being a ligand for BP-80 or a BP-80-like molecule.

MATERIALS AND METHODS

Recombinant DNA

All constructs used in this work are shown in Figure 1. All protein-coding sequences were fused downstream to the CaMV 35S promoter in expression vector pDHA (Tabe et al., 1995). The preparation of constructs for the expression of ppricin, pRTA, and pRTB has been described previously (Frigerio et al., 1998b). The C-terminal RTA-linker fusion was generated from the ppricin-coding sequence by PCR using the oligonucleotides 5′-TCTAGAATGAAACCGG-GAGGAAATACTATT -3′ and 5′-CTGCAGTCAATTA-AAATTTGGTACC3-′. The fusion between the signal peptide and the mature coding sequence of pRTB was generated by PCR using the oligonucleotides 5′-TCTGCCTCATTTGC-CTCTTTGCTTATAAGG-3′ and 5′-CCTTATAAGCAAA-GAGGCAAATGAGGCAGA-3′. mGFP5 was amplified from plasmid pGFP5-ER (a gift from J. Haseloff), and the linker peptide-coding region fused to the 3′ of GFP by PCR with the oligonucleotide 5′-CTGCAGCTAATTAAAATTTGGTAC-CACTGGCCTTATAAGCAAAGATTATTTGTATAGTTC-3′. The oligonucleotide 5′-CTGCAGCTAATTAAAATTTG-GTACCACTGGCCTTATAAGCAAAGAACCCTTTCTTCC-CTTTGC-3′ was used to fuse the ricin linker to phaseolin Δ418 (Frigerio et al., 1998b).

The Ile 271 to Gly mutation was introduced into the linker sequence of ppricin, pRTA-L, and Δ418-L by using the oligonucleotides 5′-TCTTTGCTTGGAAGGCCAGT-3′ and 5′-ACTGGCCTTCCAAGCAAAGA-3′ and the QuickChange in vitro mutagenesis system (Stratagene, La Jolla, CA), following the manufacturer's instructions.

Protoplast Transfection

Protoplasts were prepared from axenic leaves (4–7 cm long) of tobacco (*Nicotiana tabacum* cv Petit Havana SR1.) or from cultured suspension cells of Arabidopsis (Axelos et al., 1992). Protoplasts were subjected to polyethylene glycol-mediated transfection as described by Pedrazzini et al. (1997) and were incubated overnight at 25°C in the dark before pulse labeling or for 24 h at 25°C in the dark before microscopical observation.

In Vivo Labeling of Protoplasts and Analysis of Expressed Polypeptides

Pulse-chase labeling of protoplasts using Pro-Mix (a mixture of ^{35}S-Met and ^{35}S-Cys; Amersham, Buckinghamshire, UK) was performed as described (Pedrazzini et al., 1997). Where indicated cells were pre-incubated with 10 μg mL^{-1} of brefeldin A (Boehringer Mannheim, Basel) for 1 h before labeling. Homogenization of protoplasts and incubation media was performed by adding to the frozen samples 2 volumes of ice-cold homogenization buffer (150 mM Tris-Cl, 150 mM NaCl, 1.5 mM EDTA, and 1.5% [w/v] Triton X-100, pH 7.5) supplemented with complete protease inhibitor cocktail (Boehringer Mannheim). Immunoprecipitation of expressed polypeptides was performed as described previously (Frigerio et al., 1998a) using rabbit polyclonal antisera raised against RTA, RTB, GFP (Molecular Probes, Eugene, OR), or phaseolin. Immunoselected proteins were analyzed by 15% (w/v) reducing SDS-PAGE and fluorography.

Vacuole purification was performed as described (Frigerio et al., 2000). The recovery of vacuoles in the vacuolar fraction was around 15% based on α-mannosidase activity; the vacuolar fraction contained less than 1% of the total cellular amount of the ER resident chaperone binding protein, indicating very low contamination by other compartments of the secretory pathway (data not shown)

Confocal Microscopy

Arabidopsis protoplasts were transfected with GFP constructs as described (Di Sansebastiano et al., 1998). Cells were incubated in the dark for 24 h at 25°C before observation. Images were collected with a confocal laser-microscope (DMR, Leica Microsystems, Wetzlar, Germany) using an operating system (TCS 4D, Leica) with a 40× objective. A fluorescein isothiocyanate filter set was used to detect GFP fluorescence from living protoplasts. An image with transmitted light was also collected using the confocal microscope. Images were assembled with Adobe Photoshop (Adobe Systems, Mountain View, CA).

ACKNOWLEDGMENTS

We thank Alessandro Vitale, Ombretta Foresti, and Aniello Santoro for critical reading of the manuscript.

Received December 27, 2000; accepted January 12, 2001.

LITERATURE CITED

Ahmed SU, Bar-Peled M, Raikhel NV (1997) Cloning and subcellular location of an Arabidopsis receptor-like protein that shares common features with protein-sorting receptors of eukaryotic cells. Plant Physiol **114:** 325–336

Ahmed SU, Rojo E, Kovaleva V, Venkataraman S, Dombrowski KE, Matsuoka K, Raikhel NV (2000) The plant vacuolar sorting receptor AtELP is involved in transport of NH_2-terminal propeptide-containing vacuolar proteins in *Arabidopsis thaliana*. J Cell Biol **149:** 1335–1344

Axelos M, Curie C, Mazzolini L, Bardet C, Lescure B (1992) A protocol for transient gene expression in *Arabidopsis thaliana* protoplasts isolated from cell suspension cultures. Plant Physiol Biochem **30:** 123–128

Bagga S, Sutton D, Kemp JD, Sengupta-Gopalan C (1992) Constitutive expression of the β-phaseolin gene in different tissues of transgenic alfalfa does not ensure phaseolin accumulation in non-seed tissue. Plant Mol Biol **19:** 951–958

Boevink P, Martin B, Oparka K, Santa Cruz S, Hawes C (1999) Transport of virally expressed green fluorescent protein through the secretory pathway in tobacco leaves is inhibited by cold shock and brefeldin A. Planta **208:** 392–400

Butterworth AG, Lord JM (1983) Ricin and *Ricinus communis* agglutinin subunits are all derived from a single-size polypeptide precursor. Eur J Biochem **137:** 57–65

Cao X, Rogers SW, Butler J, Beevers L, Rogers JC (2000) Structural requirements for ligand binding by a probable plant vacuolar sorting receptor. Plant Cell **12:** 493–506

Di Sansebastiano G-P, Paris N, Marc-Martin S, Neuhaus J-M (1998) Specific accumulation of GFP in a non-acidic vacuolar compartment via a C-terminal propeptide-mediated sorting pathway. Plant J **15:** 449–457

Ferrini JB, Martin M, Taupiac MP, Beaumelle B (1995) Expression of functional ricin B chain using the baculovirus system. Eur J Biochem **233:** 772–777

Frigerio L, de Virgilio M, Prada A, Faoro F, Vitale A (1998a) Sorting of phaseolin to the vacuole is saturable and requires a short C-terminal peptide. Plant Cell **10:** 1031–1042

Frigerio L, Vine ND, Pedrazzini E, Hein MB, Wang F, Ma JK-C, Vitale A (2000) Assembly, secretion and vacuolar delivery of a hybrid immunoglobulin in plants. Plant Physiol **123:** 1483–1493

Frigerio L, Vitale A, Lord JM, Ceriotti A, Roberts LM (1998b) Free ricin A chain, proricin and native toxin have different cellular fates when expressed in tobacco protoplasts. J Biol Chem **273:** 14194–14199

Gomez L, Chrispeels MJ (1993) Tonoplast and soluble vacuolar proteins are targeted by different mechanisms. Plant Cell **5:** 1113–1124

Hara-Nishimura I, Shimada T, Hatano K, Takeuchi Y, Nishimura M (1998) Transport of storage proteins to protein storage vacuoles is mediated by large precursor-accumulating vesicles. Plant Cell **10:** 825–836

Hara-Nishimura I, Shimada T, Hiraiwa N, Nishimura M (1995) Vacuolar processing enzyme responsible for the maturation of seed proteins. J Plant Physiol **145:** 632–640

Harley SM, Lord JM (1985) In vitro endoproteolytic cleavage of castor bean lectin precursors. Plant Sci **41:** 111–116

Hinz G, Hillmer S, Bäumer M, Hohl I (1999) Vacuolar storage proteins and the putative vacuolar sorting receptor BP-80 exit the Golgi apparatus of developing pea cotyledons in different transport vesicles. Plant Cell **11:** 1509–1524

Holwerda BC, Padgett HS, Rogers JC (1992) Proaleurain vacuolar targeting is mediated by short contiguous peptide interactions. Plant Cell **4:** 307–318

Hung C-H, Lee M-C, Lee T, Lin J-Y (1993) Primary structure of three distinct isoabrins determined by cDNA sequencing: conservation and significance. J Mol Biol **229:** 263–267

Jiang L, Phillips TE, Rogers SW, Rogers JC (2000) Biogenesis of the protein storage vacuole crystalloid. J Cell Biol **150:** 755–769

Kervinen J, Tobin GJ, Costa J, Waugh DS, Wlodaver A, Zdanov A (1999) Crystal structure of plant aspartic proteinase prophytepsin: inactivation and vacuolar targeting. EMBO J **18:** 3947–3955

Kirsch T, Paris N, Butler JM, Beevers L, Rogers JC (1994) Purification and initial characterization of a potential plant vacuolar targeting receptor. Proc Natl Acad Sci USA **91:** 3403–3407

Kirsch T, Saalbach G, Raikhel NV, Beevers L (1996) Interaction of a potential vacuolar targeting receptor with amino- and carboxyl-terminal targeting determinants. Plant Physiol **111:** 469–474

Koide Y, Matsuoka K, Ohto M, Nakamura K (1999) The N-terminal propeptide and the C-terminus of the precursor to 20-kilodalton potato tuber protein can function as different types of vacuolar sorting signals. Plant Cell Physiol **40:** 1152–1159

Lamb FI, Roberts LM, Lord JM (1985) Nucleotide sequence of cloned cDNA coding for preproricin. Eur J Biochem **148:** 265–270

Lord JM (1985) Precursors of ricin and *Ricinus communis* agglutinin: glycosylation and processing during synthesis and intracellular transport. Eur J Biochem **146:** 411–416

Matsuoka K (2000) C-terminal propeptides and vacuolar sorting by BP-80-type proteins: not all C-terminal propeptides are equal. Plant Cell **12:** 181–182

Matsuoka K, Bassham DC, Raikhel NV, Nakamura K (1995) Different sensitivity to wortmannin of two vacuolar sorting signals indicates the presence of distinct sorting machineries in tobacco cells. J Cell Biol **130:** 1307–1318

Matsuoka K, Nakamura K (1991) Propeptide of a precursor to a plant vacuolar protein required for vacuolar targeting. Proc Natl Acad Sci USA **88:** 834–838

Matsuoka K, Nakamura K (1999) Large alkyl side-chains of isoleucine and leucine in the NPIRL region constitute the core of the vacuolar sorting determinant of sporamin precursor. Plant Mol Biol **41:** 825–835

Matsuoka K, Neuhaus J-M (1999) Cis-elements of protein transport to the plant vacuoles. J Exp Bot **50:** 165–174

Pedrazzini E, Giovinazzo G, Bielli A, de Virgilio M, Frigerio L, Pesca M, Faoro F, Bollini R, Ceriotti A, Vitale A (1997) Protein quality control along the route to the plant vacuole. Plant Cell **9:** 1869–1880

Saalbach G, Rosso M, Schumann U (1996) The vacuolar targeting signal of the 2s albumin from Brazil nut resides at the C-terminus and involves the C-terminal propeptide as an essential element. Plant Physiol **112:** 975–985

Shimada T, Kuroyanagi M, Nishimura M, Hara-Nishimura I (1997) Pumpkin 72-kDa membrane protein of precursor accumulating vesicles have characteristics for a vacuolar sorting receptor. Plant Cell Physiol **38:** 1414–1420

Tabe LM, Wardley-Richardson T, Ceriotti A, Aryan A, McNabb W, Moore A, Higgins TJV (1995) A biotechnological approach to improving the nutritive value of alfalfa. J Anim Sci **73:** 2752–2759

Van Damme EJ, Hao Q, Charels D, Barre A, Rouge P, Van Leuven F, Peumans WJ (2000) Characterization and molecular cloning of two different type 2 ribosome-inactivating proteins from the monocotyledonous plant *Polygonatum multiflorum*. Eur J Biochem **267:** 2746–2759

Van Damme EJM, Barre A, Rougé P, van Leuven F, Peumans WJ (1996) The NeuAc(alpha-2, 6)-Gal/GalNac-binding lectin from elderberry (*Sambucus nigra*) bark, a type-2 ribosome-inactivating protein with an unusual specificity and structure. Eur J Biochem **235:** 128–137

Vitale A, Raikhel NV (1999) What do proteins need to reach different vacuoles? Trends Plant Sci **4:** 149–155

von Schaewen A, Chrispeels MJ (1993) Identification of vacuolar sorting information in phytohemagglutinin, an unprocessed vacuolar protein. J Exp Bot **44:** 339–342